

Effects of film thickness on moisture sorption, glass transition temperature and morphology of poly(chloro-*p*-xylylene) film

HongLiang Huang, Yongan Xu, Hong Yee Low*

Molecular and Performance Materials Cluster, Institute of Materials Research and Engineering, 3 Research Link, Singapore 117602, Singapore

Received 8 October 2004; received in revised form 25 April 2005; accepted 17 May 2005

Available online 15 June 2005

Abstract

Moisture sorption, glass transition temperature (T_g) and morphology of ultra thin poly(chloro-*p*-xylylene) (parylene-C) are greatly influenced by geometrical confinement effects. For film <50 nm, the equilibrium moisture saturation is a decreasing function of film thickness. However, the T_g of film <50 nm is about 10 °C higher than thicker films. The above phenomena are attributed to the effect of geometrical confinement on the thermal properties and the morphology of parylene-C film. Surface confinement results in an increased in T_g , but a decreased in crystallinity for films <50 nm. In this study, we show that the increase in moisture sorption for parylene-C films <50 nm is dominated by the crystallinity variation.

© 2005 Elsevier Ltd. All rights reserved.

Keywords: Polymer thin film; Confinement effects; Moisture sorption

1. Introduction

Poly(*p*-xylylene) or commonly refers to as parylene and its derivatives have been widely used as protective coatings in microelectronic devices [1,2] and archival preservation [3] due to their outstanding properties, such as low moisture sorption, low dielectric constant and high optical transparency. Parylenes can be easily prepared by chemical vapour deposition (CVD) process, resulting in uniform, pinhole and solvent free films [4–6].

As miniaturation of device is inevitable, the thickness of the barrier film/protective coating used in these devices also shrinks, surface confinement eventually plays an important role in affecting the conformation, packing density, and the mobility of the polymer chains. Glass transition is one of the most commonly used properties to differentiate the thermal and physical stability in polymers. Keddie et al. was one of the earliest who reported anomalous T_g values as film thickness decreases below 40 nm [7]. It is now understood that when the interaction of the film with the substrate is strong, the surface confinement effect results in restricted

chain mobility, and T_g increases as film thickness decreases. On the other hand, if the film/substrate interaction is weak, the free surface effect dominates, and the polymer has higher mobility, thus a lower T_g is expected for ultra thin film [8,9]. The above thickness-dependent T_g on supported film can be described by the following equation [10]:

$$\frac{T_g(z)}{T_g(\infty)} = \frac{1}{2} \left\{ \exp\left(-\frac{\alpha_1 - 1}{z/z_0 - 1}\right) + \exp\left(-\frac{\alpha_2 - 1}{z/z_0 - 1}\right) \right\}$$

where z is the film thickness, $T_g(z)$ and $T_g(\infty)$ are the thickness-dependent T_g and the bulk value, respectively, α_1 is a measure of the free surface effect, the substrate effect is represented by α_2 , and z_0 represents a characteristic length. Thus, the thickness-dependent behaviour of T_g is determined by both the free surface effect and film/substrate interfacial effect. High chain mobility is anticipated at the free surface while restricted chain mobility at the film/surface interface when the film/substrate interaction is strong [11]. Reiter has reported that the reduction of T_g in supported polystyrene (PS) films is attributed to a reduction in mass density when the film is thinner than the average end-to-end distance [12]. Thickness dependent of T_g is also affected by the molecular weight of the polymer. Through the study of free-standing film, Mattson et al. have concluded that for thin film where the M_n is in the lower regime, the T_g is controlled by a characteristic length scale

* Corresponding author. Tel.: +65 6874 8133.

E-mail address: hy-low@imre.a-star.edu.sg (H.Y. Low).

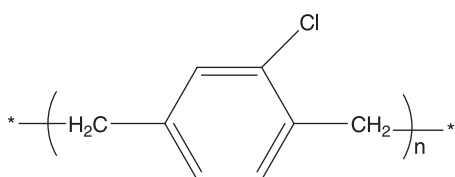
intrinsic to glass transition, while in the higher M_n regime, chain confinement dominates the T_g [13]. A model was further developed, which describes the T_g dependent behaviour of ultra thin film by combining the presence of a highly mobile free surface layer with a length scale for cooperative dynamics [14]. This model shows a qualitative agreement with experimentally observed supported and free-standing films.

The relationship between the thickness dependence T_g has also been linked to the polymer chain dynamics through diffusion of small molecules. Diffusion coefficient of dye molecules in PS film has been reported to decrease as the film thickness decreases in conjunction with a decrease in the T_g [15]. Another study on the swelling of polyelectrolyte reports that the equilibrium swelling is independence of film thickness but the diffusion coefficient decreases with decreasing film thickness [16]. The decrease in diffusion coefficient is attributed to confinement effect. In this work, we report the study of moisture absorption of parylene-C film in relation to the changes in T_g and film structure/morphology as a function of film thickness. Majority of previous studies on thin film confinement focus on thermoplastic polymers such as PS and poly(methyl methacrylate) (PMMA). Parylene-C is a linear polymer and semicrystalline in bulk phase. Also, in comparison to existing reports of thin film dynamics, parylene-C is deposited via vapour phase deposition without the effect of solvent and spin coating. The chemical structure of parylene-C is shown in Schematic 1.

2. Experimental

2.1. Parylene-C film preparation

Parylene-C films were deposited by the well-known Gorham method [4,5] using a custom designed vacuum coater. The parylene-C dimer was vaporized at 100 °C, and thermally pyrolyzed at 700 °C. The reactive intermediate was deposited and polymerized instantaneously on the substrate at room temperature in the deposition chamber. For thickness and T_g measurements, the parylene-C was deposited on cleaned Si substrate. For moisture sorption measurements, the parylene-C was deposited on the gold surface of QCM crystal. The thickness of the film was roughly controlled by the dimer feed amount.



Schematic 1. Repeat unit structure for parylene-C.

2.2. Ellipsometry measurements

Film thicknesses were measured using a variable angle spectroscopic ellipsometer VASE (J. A. Woollam Inc., Lincoln, NE). The ψ and Δ data at angles of 65, 70, 75° over the wavelength range from 500 to 1000 nm were fitted using Cauchy model. Prior to the ellipsometry measurements, the film thickness was first estimated by a KLA Tencor-P10 surface profilometer. T_g measurements were performed by placing the supported film on a Linkam TMS 94 heating/cooling stage. The ellipsometric angles (ψ and Δ) were continuously recorded at 120 s intervals while the sample was heated at a constant rate of 2 °C/min. The T_g was determined from the intersection of the best fit of two straight lines in the thickness versus temperature curve. To ensure that all samples were with equivalent and well defined thermal histories, only T_g values in the second run were used.

2.3. QCM measurements

A Maxtek research grade quartz crystal microbalance (RQCM) (PLO-10 phase lock oscillator, 5 MHz AT cut, Cr/Au polished quartz crystal, 0.4 cm² active area) was used to measure the moisture sorption. Initially, the parylene-C coated crystal sensor was allowed to reach equilibrium in a low humidity chamber (Relative humidity, RH: 20 ± 1%), then transferred immediately to a high humidity chamber (RH: 95 ± 1%). The whole moisture sorption experiment was carried out at a constant temperature of 25 ± 0.1 °C. The crystal resonance frequency was recorded at a rate of twice/min. The frequency shift was converted into mass by the following equation [17]:

$$\text{Mass} = \frac{(f_{\text{uncoated}} - f_{\text{dryfilm}})}{C_f} \quad (1)$$

where the Mass is parylene-C film mass per unit area, C_f is a constant determined by the crystal used, f_{uncoated} and f_{dryfilm} are the resonance frequencies of bare crystal and crystal coated with film (dry), respectively. The percentage of moisture absorbed at steady state can be calculated by the following equation:

$$\text{Moisture (wt\%)} = \frac{(f_{\text{dryfilm}} - f_{\text{wetfilm}})}{(f_{\text{uncoated}} - f_{\text{dryfilm}})} * 100\% \quad (2)$$

where the f_{wetfilm} is the resonance frequency of film saturated with moisture.

2.4. X-ray diffraction and X-ray reflectivity measurements

X-ray diffraction (XRD) of the parylene-C films were measured using a Bruker GADDS diffractometer Cu K α radiation and a graphite monochromator (the accelerating voltage: 40 kV; the applied current: 40 mA). The measurements were carried out at room temperature with the

following parameters: scan range, 2.5–33°; scan time, 30 min; incident angle, 1°. Distance from the X-ray source to sample was 15 cm, and 0.5 mm double pinhole collimator.

The densities of parylene-C films were investigated by high resolution X-ray reflectometry (XRR) at grazing incidence angle in the X-ray demonstration and development beamline at Singapore Synchrotron Light Source (SSLS) Center. The diffractometer is the Huber 4-circle system 90000-0216/0, with high-precision of 0.0001° step size for Ω and 2θ circles. The storage ring, Helios 2, was running at 700 MeV, typically stored electron beam current of 200 mA. X-ray beam was conditioned to select Cu $K_{\alpha 1}$ radiation (8.048 keV in photon energy) by a Si (111) channel-cut monochromator (CCM) and blocked to be 0.20 mm high in vertical direction and 8.00 mm wide in horizontal direction by a slit system. Such set-up yielded X-ray beam with about 0.005° in divergence. The detector slit was adjusted as 0.60 mm high to ensure recording all reflected photons. The typical counting time was 5 s for every step and step size varies from 0.01 to 0.001° for different samples to ensure that the oscillation in reflectivity was well recorded. Diffuse scattering at off-set angle was also measured in the range of above measurement. As it is much weaker, there is no need to correct the specular reflectivity by subtracting the diffuse scattering. The data were corrected with the finite slit height, i.e. 0.200 mm.

The X-ray reflectivity data simulations were done using simulating software M805 and LEPTOS release 2004 (Bruker). The densities of the films thicker than 40 nm were obtained through the fitting of the critical angle, while the densities of the films less than 40 nm which do not show obvious critical angles were obtained through the fitting of the amplitudes of oscillation around the critical angles in XRR curve even though the accuracy is not as good as that of fitting of the critical angle. Levenberg-Marquardt algorithm for least-square refinement on logarithm of data can be done for all samples. Final χ^2 values were typically 3×10^{-4} .

2.5. AFM measurements

Atomic force microscopy (AFM) measurements were performed using a Digital Instrumental Nanoscope IV AFM (Digital Instruments, Santa Barbara, CA). Height images were acquired under ambient conditions in tapping mode using a silicon cantilever tip (Pointprobe™ cantilever length 128 μm and a resonance frequency of 288–326 kHz).

3. Results and discussion

3.1. Moisture sorption by QCM

The parylene-C films deposited on Si substrate are fully-grown and uniform in thickness. A representative AFM

image of 8 nm parylene-C is shown in Fig. 1. Fig. 2 shows the raw dynamic resonance frequency and resistance shift versus time for the 14 nm film. The parylene-C coated QCM is allowed to stabilize for at least 1 h in a 25 °C and 20% RH chamber before switching to a 25 °C and 95% RH chamber. For all films, there is an immediate decrease in the resonance frequency when the QCM sensor coated with parylene-C film is shifted from 20 to 95% RH. This observation was reported by a moisture sorption study on photoresist films using QCM [18]. It is believed that the high sensitive QCM enables the detection of instantaneous mass uptake by the film. The mass of moisture sorption is obtained from the frequency shift according to Eq. (1). The moisture sorption isotherm for various film thicknesses is shown in Fig. 3. In the two-stage moisture sorption process, the first stage completes rather quickly in less than 10 min up to a frequency shift of 3–5 Hz. The second stage reaches final saturation much slowly compared to the first stage and appears to follow a Fickian diffusion behaviour. In bulk film studies, two-stage moisture sorption behaviour is commonly observed when there is a specific interaction between the polymer and the penetrant. However, both parylene-C and the Au substrate are hydrophobic, it is unlikely that parylene-C has a specific interaction with the absorbed moisture. Also, the first stage becomes more apparent with decreasing film thickness, we believe that the first stage is due to surface adsorption, which is not normally observed in a traditional moisture sorption isotherm. The second stage is due to the moisture diffusion from the outermost layer to the inner film. The time to reach the final saturation increases with increasing thickness; this is in agreement with classical one-dimensional diffusion-controlled moisture transport [19].

The equilibrium moisture saturation as a function of film thickness is summarized in Fig. 4. Since the first stage sorption is attributed to the surface adsorption, only the second stage sorption, which is attributed to the real

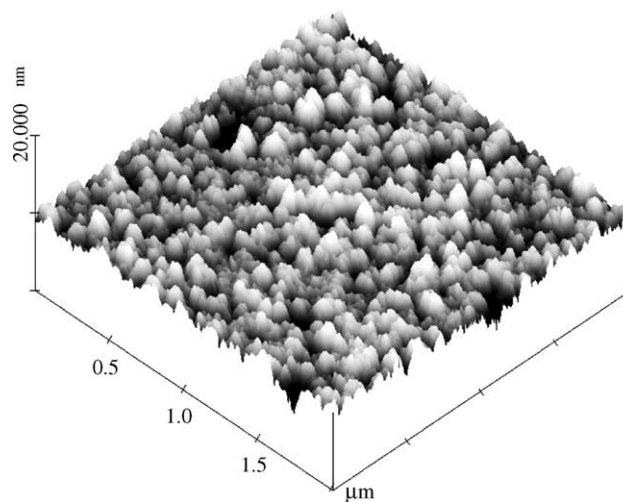


Fig. 1. AFM topographic features of the 8 nm parylene-C coated on the Si substrate.

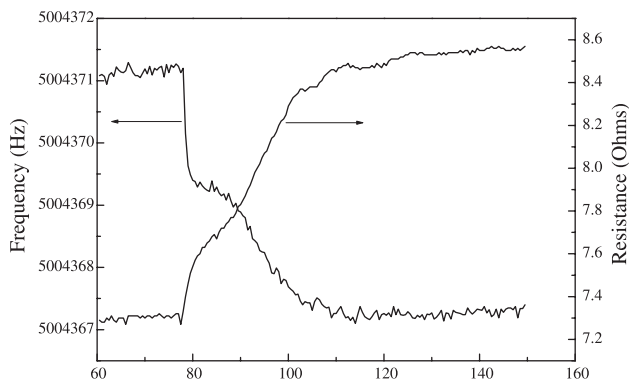


Fig. 2. Frequency and resistance change as function of moisture sorption time for the 14 nm film.

moisture sorption, is calculated. As film thickness decreases, the absolute moisture sorption (frequency change, Δf) decreases, but the equilibrium moisture sorption increases. The equilibrium moisture sorption point is exceptionally high for the 14 and 8 nm film. Water contact angle results show that the hydrophilicity of parylene-C surface is similar to that of Au surface (90° on parylene-C surface versus 84° on Au surface), eliminating the possibility of a large amount of water accumulation at the film/Au interface as reported by Vogt et al. [16] for polyimide film. Absorbed moisture calculated from QCM results is mainly attributed to real parylene-C film moisture uptake. In our study, there is no specific interaction between the parylene-C film and the substrate (Au). However, it is worth pointing out that due to the unique deposition method, the parylene-C adheres extremely well to the Au surface (attempted to peel the film off the substrate was unsuccessful). It is unlikely that the thickness dependent moisture uptake is dominated by film/substrate interaction in parylene-C. If the dynamic of ultra thin parylene-C is dominated by the confinement effect due to strong film/substrate adhesion, then a decrease in the moisture uptake is expected. Probable causes on this observation are discussed in the following sections.

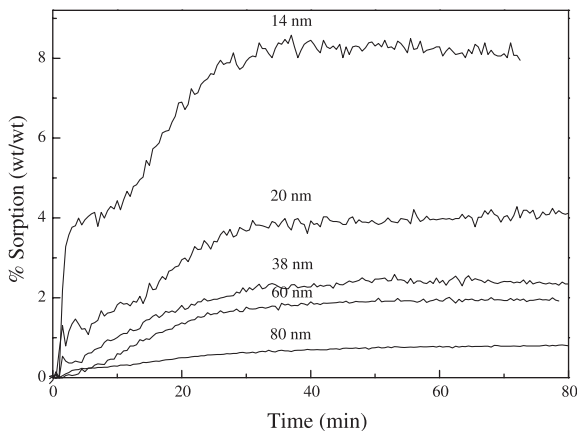


Fig. 3. Moisture sorption isotherm of parylene-C as a function of film thickness.

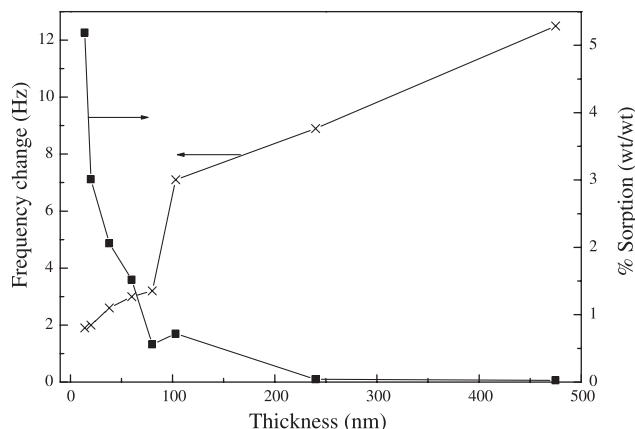


Fig. 4. Absolute and fractional moisture sorption of parylene-C films as a function of film thickness.

3.2. T_g characterization by ellipsometry

Ellipsometry has been used to yield information on the glass transition of thin film based on temperature dependence of film thickness. Fig. 5(a) shows a representative thickness and refractive index changes of a 21 nm parylene-C film as a function of temperature. The T_g value can be clearly identified from the well-defined kink. The

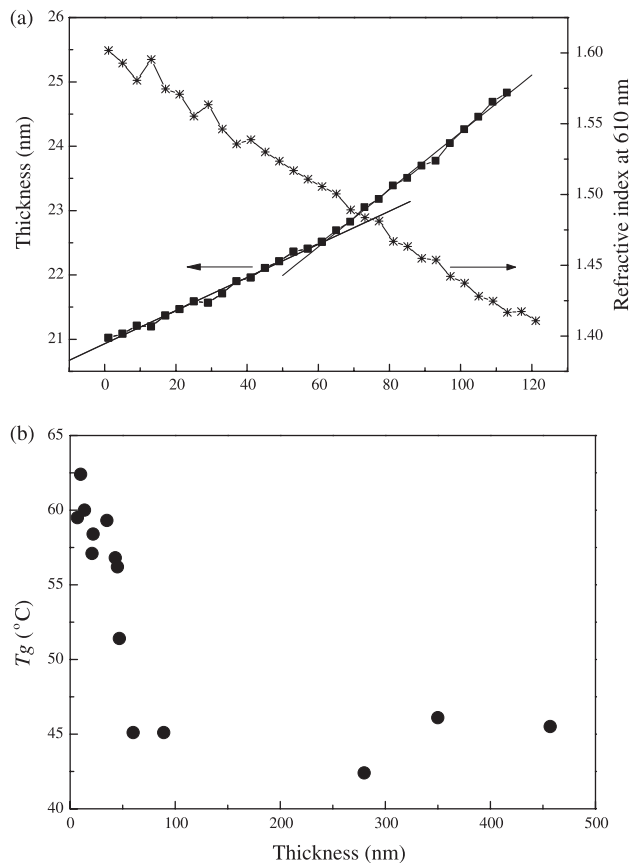


Fig. 5. (a) Representative thickness and refractive index at 610 nm changes of parylene-C film as a function of temperature. (b) T_g variation of parylene-C films as a function of film thickness.

thickness-dependence of T_g as a function of film thickness is shown in Fig. 5(b). For films thicker than 50 nm, the T_g is constant near 45 °C, in close agreement with the T_g measured by Differential Scanning Calorimetry (DSC) [20]. However, the T_g increases by about 10 °C for films thinner than 50 nm. The coefficient of thermal expansion (CTEs) of the parylene-C as a function of film thickness is plotted in Fig. 6. The CTEs below and above T_g increase as the thickness of the film decreases. As reported by Kahle et al. [21], the extraordinary enhanced CTE is mainly attributed to the temperature dependence of the optical properties of the Si substrate.

3.3. Film crystallinity and density by X-ray diffraction and reflectivity

For thinner parylene-C film, possible causes for the higher T_g , higher moisture sorption for thinner films are: (1) lower film density; (2) lower degree of crystallinity, but (3) strong film/substrate adhesion.

Fig. 7 shows that for film thinner than 50 nm, its density is substantially lower compared to thicker films as obtained from XRR. It was also confirmed by the refractive index results. For same material under same physical state, the refractive index decreases with decreasing density assuming that there is no mass loss due to thermal degradation. Indeed, QCM was used to verify that there is no mass loss of the parylene-C thin film at 140 °C. Fig. 8 shows that the refractive index at 610 nm and 25 °C decreases with decreasing thickness, indicating the density decrease. A lower density could be a result of low packing density in the amorphous phase or a lower crystallinity. Fig. 9(a) shows the XRD peak for parylene-C film with thickness ranges from 10 to 150 nm. The diffraction peak at $2\theta=14^\circ$ correspond to the (020) plane of the monoclinic unit cell, this crystal phase is also refer to as the α -phase [22]. The crystallinity was derived by normalizing the integrated peak intensity with film thickness under the assumption of there is no crystal structure change within this thickness range. As

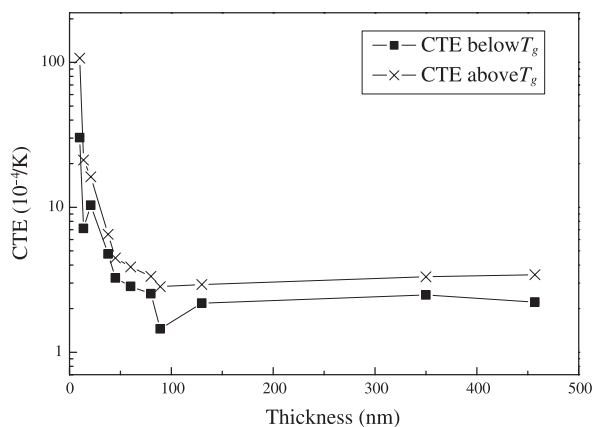


Fig. 6. CTEs below and above T_g of parylene-C films as a function of film thickness.

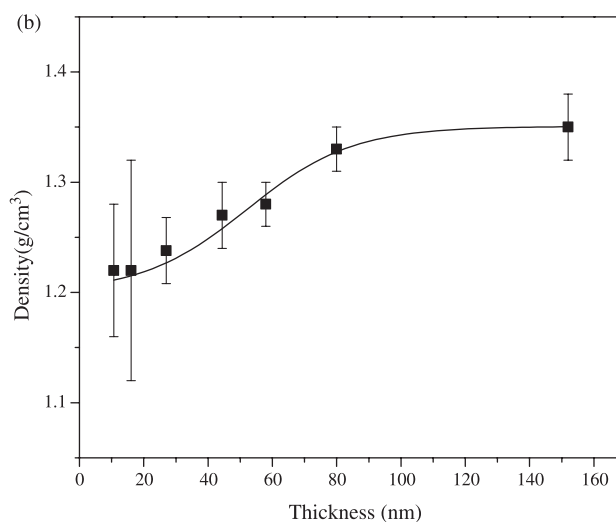
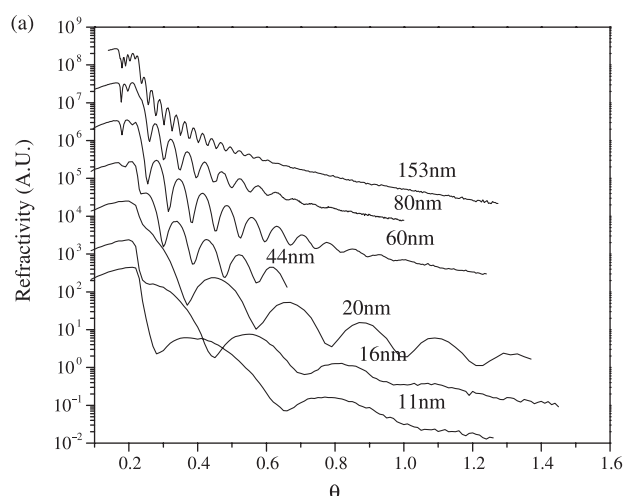


Fig. 7. (a) XRR curves for various parylene-C films. (b) Density variation of parylene-C films as a function of film thickness obtained from XRR data.

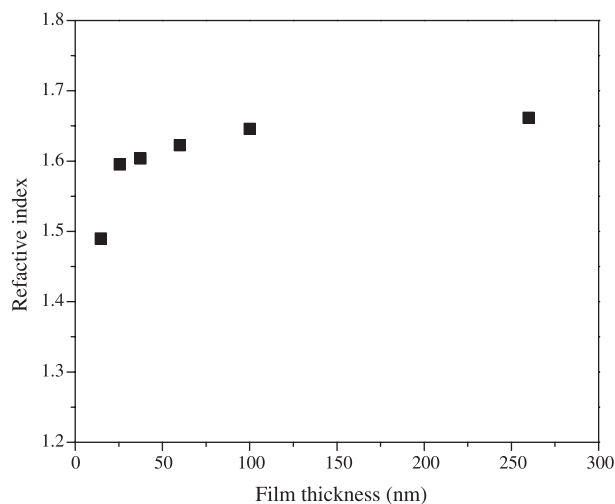


Fig. 8. Refractive index variation at 610 nm and 25 °C as a function of film thickness.

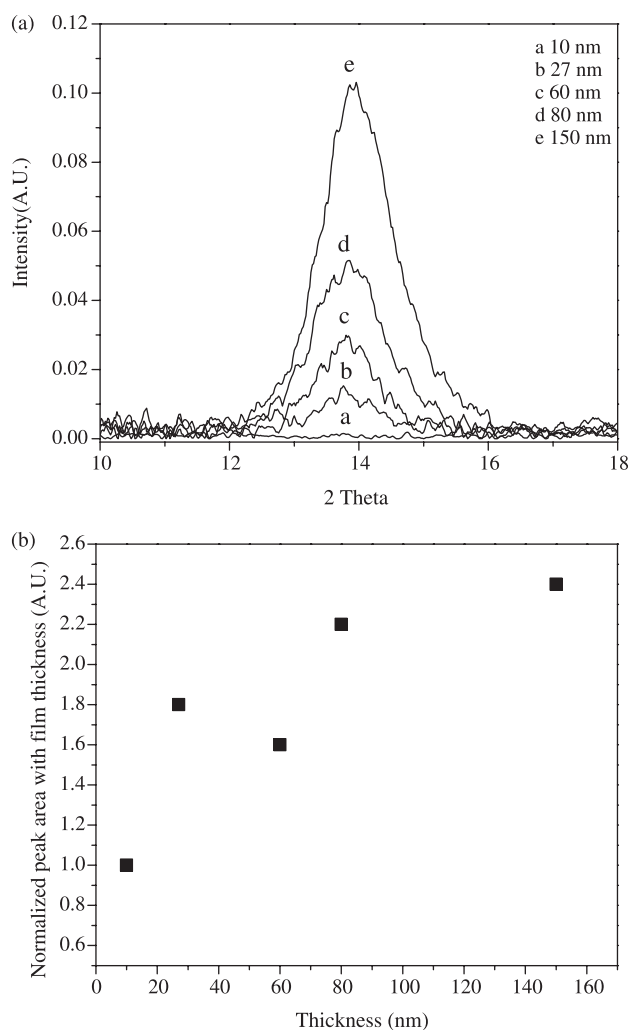


Fig. 9. (a) XRD peaks of parylene-C as a function of film thickness. (b) Normalized XRD peak intensity as a function of film thickness.

shown in Fig. 9(b), crystallinity of parylene-C shows a non-linear dependence on film thickness, specifically the crystallinity decreases as film thickness decreases. Due to the surface confinement in ultra thin film, the crystallization process as parylene-C film grows is likely to be retarded, which result in lower crystallinity. Retardation of crystallization in ultra thin film has been observed for spin coated poly(di-*n*-hexylsilane), where crystallization rate and degree of crystallinity is substantially lower when the polymer film is <50 nm [22]. A large decrease in crystallinity is observed for film below 20 nm and at ~10 nm, the film failed to crystallize. Through measurement of optical birefringence, Senkevich has shown that for parylene-C film, the crystallinity decreases significantly for film <50 nm [23]. Both AFM (Fig. 10(a)) and XRR (Fig. 10(b)) results show that the roughness of parylene-C decreases substantially when film thickness is <40 nm. The reduction in film roughness in a semicrystalline material is associated with a reduction in film crystallinity.

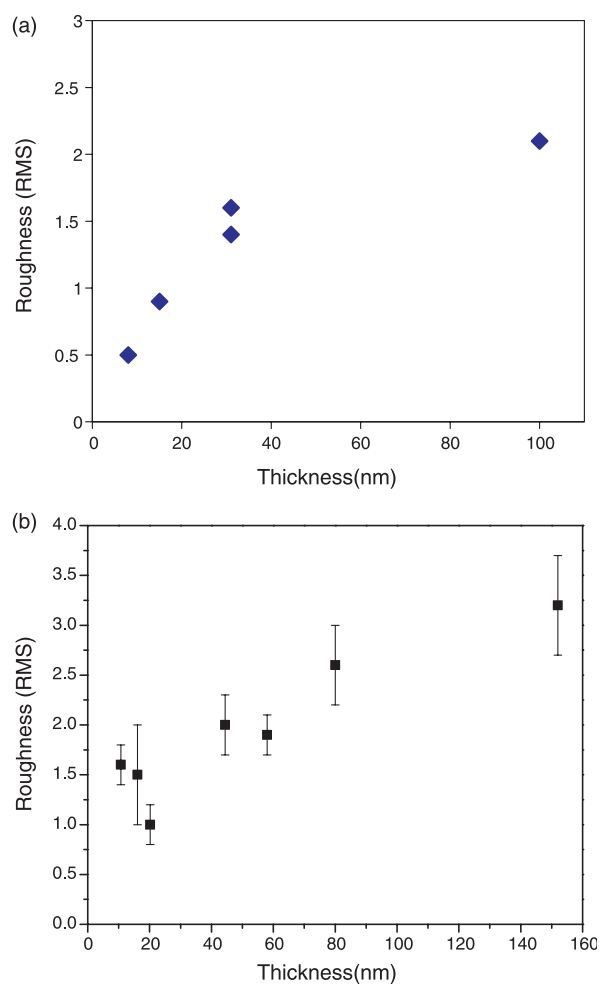


Fig. 10. (a) Surface roughness of parylene-C (from AFM scan) as a function of thickness. (b) Surface roughness of parylene-C (from XRR data) as a function of thickness.

An overall lower film density would result in higher chain mobility, however, it is worth pointing out that the moisture sorption experiment was carried with parylene-C deposited on the gold-coated quartz crystal, while the T_g measurement was carried out for parylene-C film deposited on Si wafer. Although we do not anticipate specific interaction between the parylene-C with either the gold or the Si substrate, it is possible that the Si substrate having a native oxide/hydroxide interacts with the chlorine group in parylene-C. The strong film/substrate adhesion may affect the length scale for co-operative motion of parylene-C chain, resulting in higher T_g . An increase in the percentage of the amorphous phase does not result in an increase in T_g , only an increase in the signal for T_g detection. However, since CTE is a measure of both the crystalline and amorphous phase, the higher percentage of amorphous phase results in higher CTE. In this study, we show that the moisture sorption behaviour of parylene-C as a function of film thickness is dominated by the effect of crystallinity change.

4. Conclusions

Geometrical confinement has significant effects on the moisture sorption, T_g and the morphology of ultra thin parylene-C film. The highly mass-sensitive QCM allows the monitoring of the moisture uptake of these ultra thin films over time. Interestingly, surface adsorption was discernible from the moisture sorption isotherm. In this study, we show that surface confinement has resulted in a retarded crystallization during the growth of parylene-C. The lower crystallinity in ultra thin film (<50 nm) accounts for the observed lower film density. Although the surface confinement resulted in higher T_g for film <50 nm, the overall effect of an increase in the amorphous phase dominates the moisture sorption of the ultra thin parylene-C films.

Acknowledgements

The authors thank Dr Su Xiaodi (Institute of Materials Research and Engineering) for the discussion of QCM results, Dr Yang Ping (Singapore Synchrotron Light Source) for assistance in the XRR data collection and fitting.

References

- [1] Ke L, Kumar RS, Zhang K, Chua SJ, Wee ATS. *Microelectron J* 2004; 35:325–8.
- [2] Dolbier Jr WR, Beach WF. *J Fluorine Chem* 2003;122:97–104.
- [3] You L, Yang GR, Lang CI, Moore JA, Wu P, McDonald JF, et al. *J Vac Sci Technol, A* 1993;11:3047–52.
- [4] Gorham WF. *J Polym Sci A-1* 1966;4:3027–39.
- [5] Fortin JB, Lu TM. *Chem Mater* 2002;14:1945–9.
- [6] Vaeth KM, Jensen KF. *Macromolecules* 2000;33:5336–9.
- [7] Keddie JL, Jones RAL, Cory RA. *Europhys Lett* 1994;27:59–64.
- [8] Keddie JL, Jones RAL, Cory RA. *Faraday Discuss* 1994;98:219–30.
- [9] Grohens Y, Brogly M, Labbe C, David MO, Schultz J. *Langmuir* 1998;14:2929–32.
- [10] Zhou H, Kim HK, Shi FG, Zhao B, Yota J. *Microelectron J* 2002;33: 221–7.
- [11] van Zanten JH, Wallace WE, Wu WL. *Phys Rev E* 1996;53: R2053–R6.
- [12] Reiter G. *Macromolecules* 1994;27:3046–52.
- [13] Mattsson J, Forrest JA, Bojesson L. *Phys Rev E* 2000;62:5187–200.
- [14] Forrest JA, Mattsson J. *Phys Rev E* 2000;61:R53–R6.
- [15] Tseng KC, Tarro NJ, Durning CJ. *Phys Rev E* 2000;61:1800–11.
- [16] Vogt BD, Soles CL, Lee HJ, Lin EK, Wu WL. *Langmuir* 2004;20: 1453–8.
- [17] Berger CM, Henderson CL. *Polymer* 2003;44:2101–8.
- [18] Soles CL, Jones RL, Lenhart JL, Prabhu VM, Wu WL, Lin EK, et al. *Proc SPIE* 2003;5039:366–75.
- [19] Vanlandingham MR, Eduljee RF, Gillespie Jr JW. *J Appl Polym Sci* 1999;71:787–98.
- [20] Senkevich JJ, Desu SB. *Polymer* 1999;40:5751–9.
- [21] Kalhe O, Wielsch U, Metzner H, Bauer J, Uhlig C, Zawatzki C. *Thin Solid Films* 1998;313–314:803–7.
- [22] Despotopoulou MM, Frank CW, Miller RD, Rabolt JF. *Macromolecules* 1996;29:5797–804.
- [23] Senkevich JJ. *J Vac Sci Technol A* 2000;18:2586–90.